Proceedings of the 28th IEEE
EMBS Annual International Conference
New York City, USA, Aug 30-Sept 3, 2006

A Non-Contact Imaging-Based Approach to Detecting Stage I Pressure Ulcers

Jon Leachtenauer, Steve Kell, Beverely Turner, Chris Newcomer, Courtney Lyder, Majd Alwan,
Senior Member, IEEE

Abstract— **This paper describes a non-contact imaging-based method to detect Stage I pressure ulcers over a wide range of melanin levels. Two approaches were explored: the first used broad and narrow band visible spectrum imaging, and the second used near infrared (NIR) imaging. Preliminary results are presented together with results of numerical analysis of different erythema indices derived from the visible spectrum images. The results have shown that a low-cost imaging-based approach to detecting pressure ulcers is feasible and can yield promising results when applied to subjects with darker skin pigmentation.**

***Index Terms*— Emerging Technologies, Non-Contact Imaging-based Detection Methods, Pressure Ulcer, Erythema, Dark Skin Pigmentation.**

I. Introduction

Pressure ulcers represent a costly problem affecting an estimated 1 to 3 million adults [1]. An estimated 70% of these are elderly [2]. It is reported that 50% of elderly patients will develop pressure ulcers within the first week of institutionalization [3]. The cost to heal each ulcer averages from $500 to $40,000 with an estimated cost to Medicare of $1.34 billion [1, 4]. Pressure ulcers are not only costly, but are associated with increased mortality [5].

Pressure ulcers occur when unrelieved pressure, typically over a bony protrusion, initially causes blood to pool at the site [6]. Blood vessels are constricted and the skin is starved of oxygen and other nutrients. If not diagnosed and pressure relieved, the skin or even underlying tissue and bone may ulcerate. Early detection is thus key to reducing pressure ulcer suffering and subsequent treatment costs.

Manuscript received April 22, 2006. This work was supported in part by a grant from the University of Virginia Institute on Aging

J. Leachtenauer volunteers at the Medical Automation Research Center at the University of Virginia, Charlottesville, VA 22908 USA through the Health System Volunteer Services (e-mail: jleachtenauer@adelphia.net).

S. Kell is with the Medical Automation Research Center at the University of Virginia, Charlottesville, VA 22908 USA (e-mail: swk3f@virginia.edu).

B. Turner is with the Medical Automation Research Center at the University of Virginia, Charlottesville, VA 22908 USA (e-mail: bt2h@virginia.edu).

C. Newcomer is with the University of Virginia School of Nursing, Charlottesville, VA 22908 USA (e-mail: cnewc@verizon.net)

C. Lyder is with the University of Virginia School of Nursing, Charlottesville, VA 22908 USA (e-mail: chl4n@cms.mail.virginia.edu)

M. Alwan is with the Medical Automation Research Center at the University of Virginia, Charlottesville, VA 22908 USA (phone: 434-924-2265; fax: 434-924-5718; e-mail: ma5x@virginia.edu).

Historically, Stage I pressure ulcers were detected as non-blanchable areas of erythema (redness), and a blanching erythema was noted as a precursor to a Stage I ulcer [7]. Recently, the definition of Stage I pressure ulcers has been amended by the National Pressure Ulcer Advisory Panel (NPUAP) to an observable pressure-related alteration of intact skin whose indicators as compared to an adjacent or opposite area on the body may include changes in one or more of the following: skin temperature (warmth or coolness), tissue consistency (firm or boggy feel), and/or sensation (pain, itching). The ulcer appears as a defined area of persistent redness in lightly pigmented skin, whereas in darker skin tones, the ulcer may appear with persistent red, blue, or purple hues [8]. With darker skin (due to increased melanin content), the detection of erythema becomes more difficult by unaided visual inspection and currently available techniques. A study conducted by the U.S. Centers for Medicare and Medicaid Services (formerly Health Care Financing Administration) reported that the proportion of black and Hispanic patients developing more serious Stage III and IV pressure ulcers was over twice that for white patients [9]. This suggests difficulty in early detection of pressure ulcers in darkly pigmented patients.

Several previous studies have investigated the detection of erythema for both pressure ulcer detection and cosmetics purposes. A typical model of the skin shows three layers, the outer epidermis (which contains melanin), the dermis, containing hemoglobin, and the underlying reflective collagen layer [10]. In the visible portion of the spectrum, light is absorbed by melanin and hemoglobin and reflected off the collagen layer. Oxygenated hemoglobin has absorption peaks at 542nm and 574nm; de-oxygenated hemoglobin has an absorption peak at 545nm. Melanin shows a linearly decreasing absorption function with wavelength and the slope of the function is a measure of melanin content [10]. Beyond the visible portion of the spectrum, melanin absorption continues to decrease. Hemoglobin absorption increases over the range of 700-1000nm [11]. Detection of subcutaneous hemoglobin is thus most likely in the green portion of the spectrum (hemoglobin absorption peaks) and the near-infrared (NIR).

In a study of erythema detection algorithms for pressure ulcer detection using tissue reflectance spectroscopy (TRS), Riordan et al [10] found good sensitivity (0.852) and specificity (0.744) for dark-skin subjects using an algorithm developed by Diffey [12]. Sensitivity probabilistically measures the algorithm's ability to correctly detect pressure ulcers, or true positives, where as specificity characterizes

the algorithm's ability to correctly identify the lack of pressure ulcers, or true negatives. The algorithm compared reflectance in the red (635nm) and green (565nm) portions of the spectrum on the premise that an increase in erythema would increase green absorption with little increase in red. TRS is non-invasive, but requires an expensive spectrophotometer and the tools to store and analyze the resultant data and may also entail contact with the skin.

Several investigators have developed erythema meters using either white light with narrow-band filters [13] or light emitting diodes in the red and green portions of the spectrum [14]. These meters provide some quantitative measure of erythema, but require skin contact, albeit with slight pressure. They also tend to measure before and after situations such as measuring the effectiveness of UV exposure or erythema reduction treatment.

A system using a video microscope and an input/output device called a Dermascope coupled to a Personal Computer (PC), has also been developed as an erythema measurement tool [15]. A CCD camera records an image of the skin. A Dermaspectrometer was used for data comparison. The Dermaspectrometer uses two diodes emitting light centered on 568nm (green) and 655nm (red). The device displays melanin (red absorption) and erythema (red/green absorption difference) indices defined as:

$$Melanin = 100 * \log_{10}\left(1 / R_{655} \right) \quad (1)$$

$$Erythema = 100 * \left[\log_{10}\left(1 / R_{568} \right) - \log_{10}\left(1 / R_{655} \right) \right] \quad (2)$$

The CCD-defined red-green absorbance difference was measured *in vivo* on samples of UVB-induced erythema and tanning. A strong correlation was shown with the Dermaspectrometer erythema and melanin indices.

In addition to changes in the spectral response, erythema has also been shown to exhibit a temperature difference [16]. A comparison of Stage I ulcer sites with adjacent healthy tissue showed both increases and decreases in temperature. In the early stages of the current study, we briefly tested a MWIR (3-5μ) and LWIR (8-14μ) sensor, both uncooled. We abandoned this approach for reasons of both cost and variability in the temperature effect.

In keeping with its Eldercare technologies program, the Medical Automation Research Center (MARC) undertook a pilot study of erythema detection in the presence of high melanin levels. The ultimate goal of this project is to develop a low-cost, non-contact imaging-based erythema detection system that would enhance the nursing staff's ability in detecting Stage I pressure ulcer in populations with darker skin pigmentation. Two approaches were taken: the first explored visible spectrum imaging, both broad and narrow band, while the second explored NIR imaging.

II. METHOD

Reactive hyperemia was induced in twenty subjects using a simple indenting mechanism. The indented area was imaged with an unfiltered digital camera (RGB), a filtered digital camera, and a NIR camera. Images were inspected to assess the ability to detect erythema. Melanin and erythema index values were computed using processed RGB images.

A. Subjects

A sample of 20 subjects was used. Subjects were recruited based on skin color as defined by an experienced clinician. Skin color was classified as black, dark brown, brown, light brown, and pink. Four subjects were recruited for each category. Twelve subjects were male and eight were female. All subjects signed an IRB-approved informed consent form and were compensated for their participation. The experimental and data collection procedure took less than 30 minutes per participant.

B. Indenting Procedure

A 12mm sphere was used for indenting. The sphere (a glass marble) was placed in a hemispherical cavity mounted on a platform where the height could be adjusted. The subjects were instructed to place the back of their upper arm on the sphere at a point ~50mm beyond the point of the elbow and to keep their upper arm horizontal and their lower arm vertical. The weight of the arm supplied the indenting pressure (estimated as 50 mm Hg); subjects were instructed not to press on the marble. A two-minute indenting period was used. At the end of the period, the arm was placed horizontally on the platform for imaging with the forearm at an angle of 60 degrees or more relative to the upper arm. The clinician inspected the indent site before and after indentation and noted visible changes due to indenting.

C. Imaging Procedure

A digital camera (3.8 mega pixel CCD array with a response from ~ 400 nanometers to 850 nanometers) was used to acquire images in the visible region. RGB images were acquired in JPEG format (1067 x 768) and also processed to three TIFF grayscale images (red, green, and blue layer). Images were also acquired with three narrow bandpass interference filters; a red filter (636nm) and two different green filters (500 and 568nm). The center wavelength tolerance was specified as ± 2nm and the FWHM as 10nm with collimated input. The filtered images were converted from RGB images to grayscale images.

Florescent overhead lighting was employed for the unfiltered images and the camera flash plus a supplemental flash were used for the filtered images. Exposures were set to
avoid saturation while maintaining dynamic range. Imaging distance was ~1m.

The IR images were acquired with an IR video camera containing a Samsung 1/3" chip. Three IR LEDs were mounted on each side of the camera lens. A Wratten 87B filter was placed over the lens and LEDs. The cost of the IR imaging system was less than $100.

Before indenting, the target indent area was imaged with the visible camera with and without filters and the IR camera. The forearm of the target area was also imaged with the unfiltered visible camera and the IR camera. The target area was then indented and imaged again with the visible unfiltered and visible filtered camera and IR camera. The

process was then repeated for the other arm for a total of 24 imaging operations for each subject. A three level step wedge was included in all images. This provided for a relative reflectance calibration as well as an indication of dynamic range.

D. Image Processing

For each IR imaging sequence, three successive frames were extracted and averaged to improve signal-to-noise ratio. The unfiltered visible images were saved as RGB (color) images and the R, G, and B layers as gray scale images. The red layer of the red filtered image (636nm) and the green layer of the green filtered image (568nm) were saved as gray scale images, the 500nm image was not used due to lower contrast.

All the acquired images covered more than just the target area of interest. For viewing and display, a histogram of the imaged upper arm area was generated. Pixel values corresponding to the 0.05 and 99.95 percentiles were defined and the images were expanded to this range.

E. Image Display

The processed images were initially reviewed to assess the relative performance of the different imaging modalities. The images will ultimately be reviewed by a sample of clinician observers in a blind test to assess the sensitivity and specificity of each imaging modality and any enhancements that will subsequently be applied to these images.

F. Image Analysis

Analysis has been performed on the broadband red and green gray scale image. For each post-indentation image, a luminance histogram was generated for three non-indented areas in close proximity to the indented area.

The values were normalized relative to the white reflectance target and a melanin index computed as in (1) previous and an erythema index as in (2) where R_r and R_g are the normalized red and green reflectance values substituted for R_{655} and R_{568} respectively.

III. Results

A review of the displayed images indicated that the indented areas showed greatest contrast in the broadband green layer images; good contrast was also evident on the processed broadband RGB images (Fig. 1). The IR images showed less contrast, although vein patterns were clearly evident in the forearm images (Fig. 2). All images in the figures were taken of a subject classified in the black skin category. The filtered images showed that the filters were in fact not narrow band with uncollimated light since energy was evident outside the filters' specified passbands.

The remainder of the analysis reported here focuses on numerical analysis of the broadband red and green layer images. This analysis was performed on the original unprocessed images (before histogram expansion). The effect of post-processing of the broadband color images is described in [17].

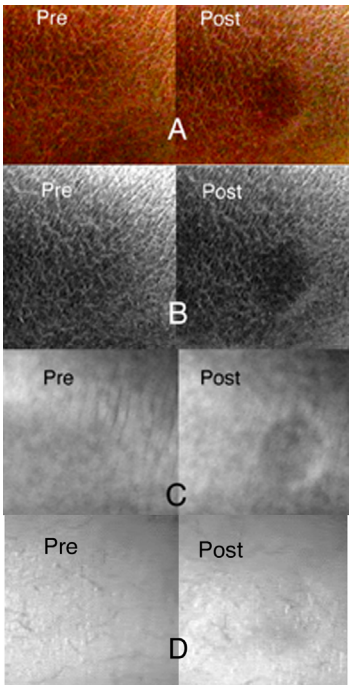

Fig. 1. Pre and post indent sites for a subject classified into the black skin category: (A) broadband RGB, (B) broadband green layer, (C) green layer of 568nm image, and (D) IR image.

Fig. 2. Broadband RGB (top) and IR image of forearm.

Analysis of variance on the melanin index data showed a statistically significant group effect; all skin color groups were significantly different from each other with the exception of the black and dark brown categories.

Indenting increased the erythema index, but also increased the melanin index. The effect was related to the original melanin index value. A so-called corrected erythema index was computed to account for this effect. It was defined as:

$$E_{adj.} = 100 * \left[\log_{10}\left(1/R_g \right) - 1.1 * \log_{10}\left(1/R_r \right) \right] \quad (3)$$

The uncorrected erythema index showed an R^2 correlation value of 0.25 with the melanin index, compared to an R^2 of 0.01 for the corrected value. Finally, the difference in green absorption was used as a measure of erythema for green layer images:

$$A_g = 100 * \log_{10}\left(1/R_g \right) \quad (4)$$

Using the broadband data, the erythema index was computed for the indented and a non-indented control site. A paired *t*-test showed that the two sets of erythema index values were significantly different ($p<0.001$, two-tailed) for all subjects. Data from the three darker skin categories (n=12) also showed significant differences ($p<0.001$, two-tailed) in the erythema index values before and after indentation, although the expert clinician had difficulty in identifying the indentation mark visually on some of these subjects.

Sensitivity and specificity values were computed for each of the aforementioned indices. A percentage difference between the erythema index of the indent site and the three non-indent (control) sites provided true positive and false negative values using difference threshold values of 5, 10, and 15%. Results are presented in Table I for all subjects (n=20) and for those in the three darkest-skin categories (n=12). In the detection of pressure ulcers, Riordan et al [10] considered sensitivity to be more important than specificity.

TABLE I
SENSITIVITY/ SPECIFICITY RESULTS

Index/ Group	Sensitivity/ Specificity		
	5%	10%	15%
E-all	0.95/ 0.82	0.87/ 0.94	0.76/ 0.96
E-dark	0.88/ 0.63	0.74/ 0.67	0.64/ 0.73
$E_{adj.}$-all	0.94/ 0.8	0.88/ 0.91	0.80/ 0.96
$E_{adj.}$-dark	0.86/ 0.54	0.76/ 0.70	0.63/ 0.77
A_g-all	0.94/ 0.85	0.83/ 0.93	0.70/ 0.97
A_g -dark	0.89/ 0.79	0.68/ 0.96	0.52/ 0.96

IV. DISCUSSION AND CONCLUSIONS

All three erythema indices showed significant increase as a function of indenting over a wide range of melanin levels; none stood out as consistently superior. Sensitivity and specificity values were comparable to those reported in [10] using TRS. Results of the current study indicate that erythema can be detected with relatively simple and low-cost imaging and image processing techniques, even in the presence of high melanin levels. Aside from the cost of a computer and display, we anticipate the cost of a detection system to be in the range of $500 to $1000.

Results also suggest possible improvements to the imaging techniques, such as a more uniform lighting arrangement, to improve the detection accuracy. This could be achieved simply by either using a smaller field of view with the lighting coupled to the lens axis or by using two orthogonal light sources. CCD cameras have an unequal and overlapping RGB response. In the current study, no attempts were made to precisely calibrate the imaging system or processes other than a relatively crude normalization process; a more rigorous calibration procedure (and filtering) is expected to improve the results.

The method presented here used numerical analysis without any image enhancement and was based on the observer's knowledge of presence of indentation and its relative location. The ability of a sample of observers to detect the same evidence on different imaging modalities, enhanced using various techniques, remains to be determined in future analysis.

ACKNOWLEDGMENT

We would like to thank the University of Virginia Institute on Aging for support of this study. We are grateful to our research participants. We would also like to thank Matt Wolfe for his effort on the project.

REFERENCES

[1] Agency for Health Care Policy and Research. Pressure ulcers in adults: prediction and prevention, US Department of Health and Human Services, Public Health Service, Rockville, Md., 1992 Pub Nos. 92-0047, 92-0050.

[2] Barbenel, J.C., Jordan, M.N., Nicol, S.M., Incidence of pressure sores in the greater Glasgow, Lancet 1977:2:248-550

[3] Oot-Giromini B, Bidwell FC, Heller NB, Parks ML, Wicks P, Williams PM. Evolution of skin care: pressure ulcer prevalence rates pre/post intervention. Decubitus 1989;2(2):54-55.

[4] Lyder, C. Exploring pressure ulcer prevention and management. JAMA 2003;248: 223-226.

[5] Allman R. The impact of pressure ulcers on health care costs and mortality. Adv Skin and Wound Care 1998;11 (3 suppl).

[6] National Pressure Ulcer Advisory Panel. Stage I definition.1998 www.npuap.org

[7] Lyder, C. Conceptualization of the Stage I pressure ulcer. J ET NURS 1991;18:162-165.

[8] Ayello EA, Henderson C, Bennett A, Sprigle S, Sussman C, Merkle D, Lyder CH, Woodruff L, Dungog EF. Stage I assessment in darkly pigmented skin. National Pressure Ulcer Advisory Panel Position Statement.www.npuap.org.

[9] Lyder C, Preston J, Scinto J, Grady J, Ahearn D. Medicare quality indicator system: Pressure ulcer prediction and prevention module: Final report. U.S. Health Care Financing Administration, November 1998.

[10] Riordan B, Sprigle S, Linden M, testing the validity of erythema detection algorithms. VA J Rehab Rehabil Res 2000:38(1)

[11] Zharov V, Ferguson S, Eidt J, Howard P, Fink L, Milton W, Infrared Imaging of Subccutaneous Veins, Lasers in Surgery and Medicine 34:56-61, 2004

[12] Diffey B and Farr P, Quantitative aspects of ultraviolet erythema, Clin. Phys. Physiol. Meas. 1991, Vol. 12, No. 4, 311-325

[13] Diffey B, Oliver R and Farr P, A portable instrument for quantifying erythema induced by ultraviolet radiation, British Journal of Dermatology, 111, 663-672, 1984.

[14] Feather J, Ellis D, and Leslie G, A portable reflectometer for the rapid quantification of cutaneous haemoglobin and melanin, Phys. Med. Biol, 1988, Vol. 33, No.6, 711-722.

[15] Takiwaki H, Shirai S, Kanno Y, Watanabe Y, and Arase S, Quantification of erythema and pigmentation using a videomicroscope and a computer, British Journal of Dermatology, 131, 85-92, 1994.

[16] Linden, M. and Sprigle, S. Skin Temperature Measurement to Predict Incipient Pressure Ulcers, Center for Rehabilitation Technology, Helen Hayes Hospital, 2004.

[17] Rajendran, P., Leachtenauer, J., Kell, S., Turner, B., Newcomer, C., Lyder, C., Alwan, M., Improving the detection of Stage I pressure ulcers by enhancing digital color images, Accepted at the 28th Annual International Conference, IEEE Engineering in Medicine and Biology, New York, 2006.